Materials Science & Engineering A 606 (2014) 40–45

Contents lists available at ScienceDirect

Materials Science & Engineering A

journal homepage: www.elsevier.com/locate/msea

Fracture toughness of a welded super duplex stainless steel

Johan Pilhagen [a,*], Henrik Sieurin [b], Rolf Sandström [a]

[a] Department of Materials Science and Engineering, KTH Royal Institute of Technology, Stockholm, Sweden
[b] Scania CV AB, Södertälje, Sweden

ARTICLE INFO

Article history:
Received 8 November 2013
Received in revised form
6 March 2014
Accepted 8 March 2014
Available online 19 March 2014

Keywords:
Duplex stainless steel
Super duplex
Fracture toughness
Weldments
Post-weld heat treatment

ABSTRACT

Fracture toughness testing was conducted on standard single-edge notched bend bar specimens of base and weld metal. The material was the SAF 2906 super duplex stainless steel. The aim was to evaluate the susceptibility for brittle failure at sub-zero temperatures for the base and weld metal. The base metal was tested between −103 and −60 °C and was evaluated according to the crack-tip opening displacement method. The fracture event at and below −80 °C can be described as ductile until critical cleavage initiation occurs, which caused unstable failure of the specimen. The welding method used was submerged arc welding with a 7 wt% nickel filler metal. The welded specimens were post-weld heat treated (PWHT) at 1100 °C for 20 min and then quenched. Energy-dispersive X-ray spectroscopy analysis showed that during PWHT substitutional element partitioning occurred which resulted in decreased nickel content in the ferrite. The PWHT weld metal specimens were tested at −72 °C. The fracture sequence was critical cleavage fracture initiation after minor crack-tip blunting and ductile fracture.

1. Introduction

Duplex stainless steels are often used in applications that require high corrosion resistance and mechanical strength. Examples are pipelines for the offshore industry, production equipment for the pulp and paper industry and pressure vessels [1]. Nowadays, there is also an increasing use of duplex stainless steel for structural applications, particularly for the grades with lower nickel and molybdenum content [2,3].

The duplex stainless steels are graded from the lean duplex (lower nickel and molybdenum content) to the "standard" grade 2205, then to the super duplex grades and nowadays to the hyper duplex grades. Super duplex stainless steels are defined by having a pitting resistance equivalent number (PRE) larger than 40. The PRE number is defined as a function of the chromium, molybdenum and nitrogen content [1].

The use of the duplex stainless is usually limited to an upper and lower service temperature. At prolonged aging at elevated temperatures (>250 °C) the duplex stainless steels exhibit a ductile to brittle transition with time. A similar ductile to brittle transition also occurs at sub-zero temperatures (°C) where the ferrite becomes increasingly brittle with decreasing temperature. The temperature for the ductile to brittle transition depends for example on the chemical content, the ferrite phase content and microstructure. Fracture toughness testing of lean duplex and the 2205 duplex stainless steel at sub-zero temperatures shows that both the base metal (hot-rolled) and weldments have satisfactory toughness down to −100 °C [4,5].

Sandvik SAF 2906 is a super duplex stainless steel specially suited for applications in caustic environments with a nominal PRE of 41. The nominal composition is (in wt%) 29 chromium, 6 nickel, 2 molybdenum and 0.4 nitrogen. Mechanical properties at room temperature conditions are yield strength of 650 MPa, tensile strength of 900 MPa and area elongation of 25%. The ductile to brittle transition temperature for impact toughness specimens occurs at −100 °C.

The purpose of this work was to evaluate the base and weld metal susceptibly for brittle failure at sub-zero temperatures for the super duplex stainless steel SAF 2906. The methods used were fracture toughness testing on standard single-edge notched bend bars specimens and the use of scanning electron microscopy (SEM) to identify the fracture mechanisms.

2. Material and fracture toughness testing

2.1. Material and welding

The material used in this work was commercially produced duplex stainless steel designated SAF 2906 (EN 1.4477, UNS S32906), produced by Sandvik Materials Technology. The product form was a 200 mm diameter bar that had been solution treated at

* Corresponding author. Tel.: +46 8790 6252.
E-mail address: pilhagen@kth.se (J. Pilhagen).

http://dx.doi.org/10.1016/j.msea.2014.03.049
0921-5093/

Table 1
Nominal chemical composition (wt%) of the plate, filler metal and the welding flux.

		Fe	Cr	Ni	Mo	Mn	N	Si	C
Bar	SAF 2906	Bal.	29	7	2.2	< 1.2	0.4	< 0.8	< 0.025
Filler metal	Sandvik 29.8.2.L, ∅ 2.4 mm	Bal.	29	7	2.4	1.0	0.36	0.4	< 0.025
		SiO_2	CaF_2	AlO_3					
Welding flux	Sandvik 15 W	7	50	40					

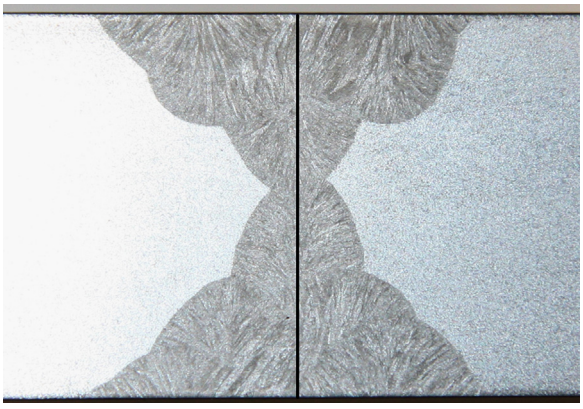

Fig. 1. Cross-section of a weldment. The black straight line shows the location of the notch and fatigue pre-crack.

Table 2
Welding parameters.

Welding method	Root gap (mm)	Land (mm)	Groove angle	Heat input (kJ/mm)	Current (A)	Voltage (V)	Welding speed (mm/min)
SAW	0	4	90°	1.6/1.9	310/360	30	350

Table 3
Amount of ferrite (a) in base metal and weldment. Automatic image analysis based on ASTM E1245 [6].

	α-Content (vol%)	Standard deviation (vol%)
Base metal	51.7	1.6
Weld metal	54.6	1.6

1100 °C and water quenched. 30 mm thick plates were extracted so that the longest side of the plate was parallel to the bar length. The chemical composition for the plate, filler metals and welding flux (which was basic) is shown in Table 1.

The weldment was produced in X-joint configuration, see Fig. 1, where the welding direction was parallel to the grain flow of the parent plates. A total of 12 beads of filler metal were used.

The temperature of the plate was held below 120 °C at all times. The welding parameters can be found in Table 2.

The welded plates were post-weld heat treated (PWHT) at 1100 °C for 20 min. The phase content in the base and weld metal was close to 50% ferrite and 50% austenite, see Table 3.

The microstructure for the base metal consisted of a ferrite matrix with austenite elongated parallel to the grain flow along the bar axis. The orientation of the crack-tip and fracture direction in relation to the microstructure is shown in Fig. 2a. For the weld metal the microstructure can be described as austenite grains in a ferrite matrix, see Fig. 2b.

No intermetallic phases were observed in the base or in the weld metal. In particular, no sigma phase was found.

2.2. Fracture toughness testing

For the fracture toughness measurement, standard single-edge notched bend bars specimens, SE(B), were used. For the base metal specimens, the dimension was $30 \times 60 \times 400$ mm^3 (thickness × width × length). For the welded specimen, the dimension was $28 \times 60 \times 290$ mm^3 and the notch-tip was located in the weld metal center line [7] as shown in Fig. 1. Side-grooves were used on all fracture toughness specimens. The crack length (nine point average) divided by the specimen width was (including fatigue pre-crack) 0.54 for the base metal and 0.49–0.51 for the welded specimens. The fracture mechanic testing was made with a 100 kN hydraulic testing machine with a clip-gauge to measure the crack mouth opening displacement (CMOD) of the specimen. The specimens were submerged in ethanol during the testing. Liquid nitrogen was used to cool the ethanol down to the testing

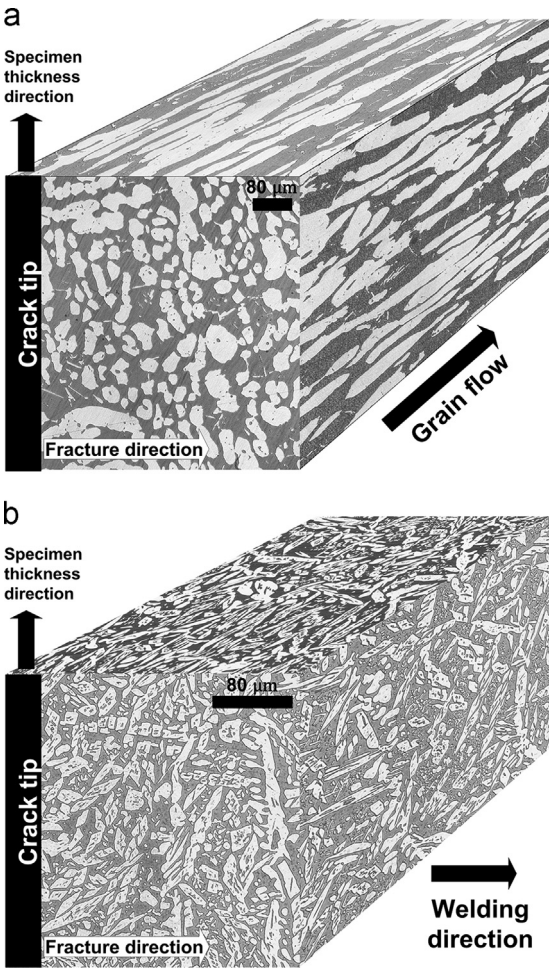

Fig. 2. Pseudo-three-dimensional representation of the microstructure: (a) base metal (100× magnification) and (b) weld metal (200× magnification).

temperature. The temperature was held constant, ±1 °C for 36 min prior to testing.

The specimens were loaded with a constant displacement rate of 0.025 mm/s until failure occurred or the test was stopped by the operator. The fracture toughness testing was based on BS7448 Part 2 [7] and ASTM E 1820-06 [8]. The fracture toughness evaluation followed ASTM E 1820-06 [8].

3. Results

Four base metal specimens were tested at temperatures between −103 and −60 °C. The specimen at −60 °C was stopped after reaching maximum force plateau and the other three specimens failed in an unstable way. The fracture surface of the specimens that failed unstably was flat with no signs of ductile fracture except for the crack-tip blunting. No large cleavage facets were visible and the surface had an opaque appearance. The fracture toughness was evaluated according to the crack-tip opening displacement (CTOD) method [8]. The yield and tensile strength used for the evaluation were obtained from a cubic polynomial fit of the data in Table 4.

The evaluated CTOD for the base is shown in Fig. 3. The attainment of maximum force plateau has been removed from the test standard as a valid failure criterion [9] and is only shown for comparison.

Observation of the fracture surface with scanning electron microscope (SEM) revealed that at and below −80 °C the specimens failed with transcrystalline cleavage after crack-tip blunting and microvoid and coalescence (MVC) fracture. The distance of ductile fracture until the unstable fracture started was of the order of 200 μm, see Fig. 4a and b.

All the weld specimens were tested at −72 °C. The straightness of the pre-crack for most of the weld metal specimens failed to meet the requirements in the test standard. All specimens had a thumbnail shape where two had a valid pre-crack shape, see Fig. 5.

Table 4
Yield and tensile strength used for the evaluation of CTOD.

Temperature (°C)	$R_{p0.2}$ (MPa)	R_m (MPa)
23	625	828
0	672	874
−25	723	924
−50	774	974
−100	876	1075
−130	938	1135

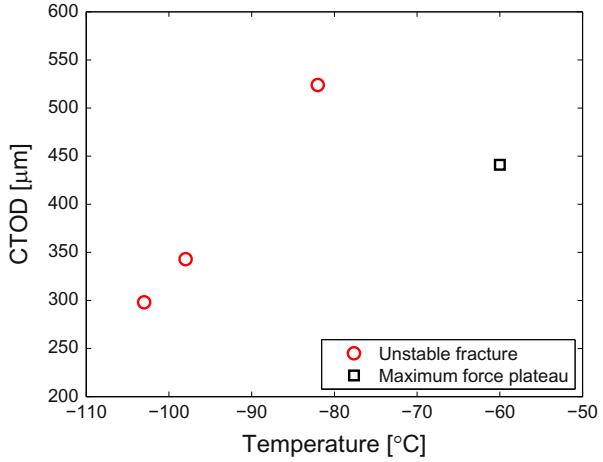

Fig. 3. Evaluated fracture toughness of the base metal.

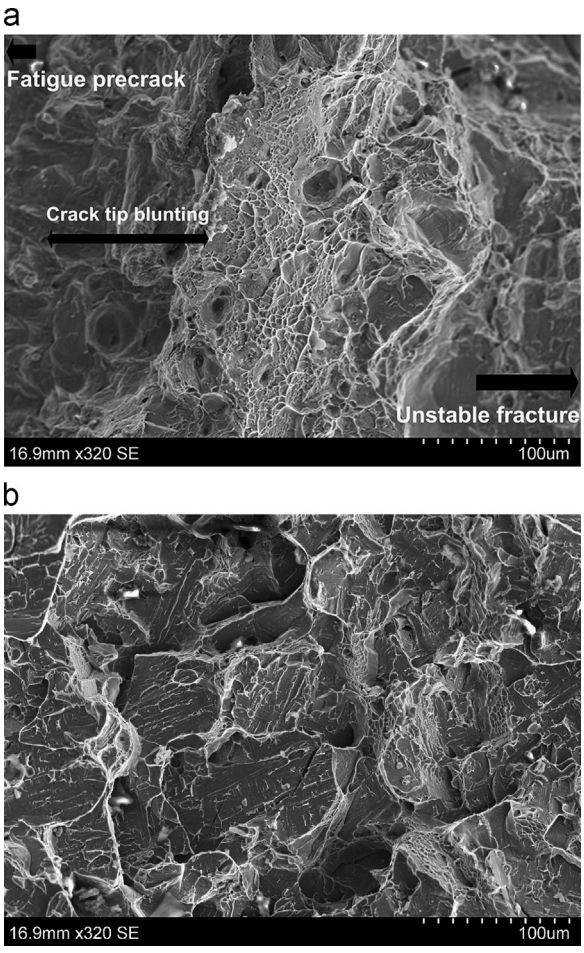

Fig. 4. Scanning electron microscopy photos of the fracture surface of the base metal: (a) crack-tip blunting and ductile fracture prior to critical cleavage fracture and (b) transcrystalline cleavage fracture.

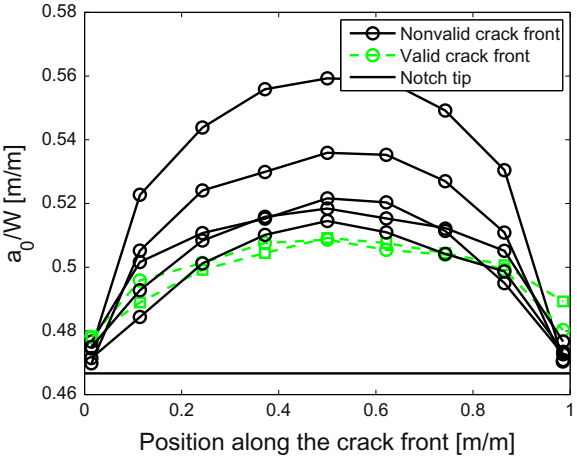

Fig. 5. Shape of the pre-crack front of the tested weld metal specimens.

All but one specimen were locally compressed for compensating the residual stress state usually found in weldments [10]. This had however no influence of pre-crack shape as the specimen with no local compression had the second highest degree of thumbnail shape. The crack length used for the fracture toughness evaluation was the nine point average stated in [8].

The evaluated fracture instability toughness determined by the *J*-integral for the weldment is shown in Table 5. The critical cleavage fracture initiation occurred after very little crack-tip

Table 5
Evaluated fracture toughness of the weld metal.

J_c (kN/m)	Max a_0/W (m/m)
27.4	0.56
53.4	0.52
43.0 (valid)	0.51
49.7 (valid)	0.51
36.2	0.52
49.3	0.51
48.2	0.54

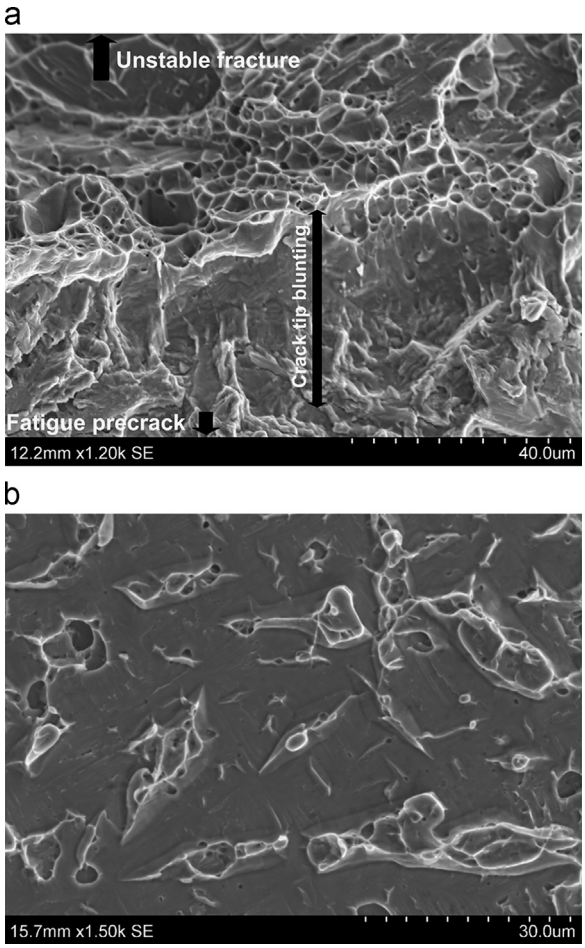

Fig. 6. Scanning electron microscope photos of the fracture surface of the weldments: (a) overview of the crack-tip and (b) the unstable fracture. Ferrite is the dark matrix and the brighter phase is austenite.

blunting and ductile fracture, see Fig. 6a. The unstable fracture occurred by transcrystalline cleavage in the ferritic phase ductile fracture in the austenite, see Fig. 6b.

4. Discussion

4.1. The base metal

For the SAF 2906 alloy, the chromium and nitrogen contents are significantly higher than for e.g. the standard 2205 alloy, 29 wt % Cr compared to 22 wt% Cr and 0.4 wt% N compared to 0.15 wt% N. Nitrogen raises the yield strength of the material. However, the solubility of the nitrogen is higher in the austenite compared to the ferrite so the nitrogen content is highest in the austenite [1]. This can cause the austenite to have a higher yield strength compared to the intrinsic stronger ferrite [11]. Microhardness measurements of the SAF 2906 alloy show that the austenite is harder than ferrite in the pristine condition and becomes significantly harder after extensive straining [12]. It has also been observed for cast duplex stainless steel that at very high nitrogen content, ~0.6 wt%, the austenite can exhibit cleavage-like fracture [11]. To evaluate whether the austenite has contributed to the unstable failure, energy-dispersive X-ray spectroscopy (EDS) analysis of the fracture surface was conducted to distinguish between the two phases. First the typical chemical composition of the two phases had to be determined from EDS analysis of a polished and etched sample, see Table 6. Unfortunately, quantitative analysis of the nitrogen content could not be done with the equipment used. Instead the nickel and molybdenum contents were used. High nickel content together with low molybdenum content indicates austenite and vice versa indicates ferrite.

Random locations of the fracture surface were used for analyzing the chemical composition of the fracture features. All cleavage fracture regions had high molybdenum content and low nickel content, cf. Table 6. Regions with high plastic deformation and signs of MVC fracture had higher nickel content and low molybdenum content comparable with Table 6. This indicates that the cleavage fracture occurs in the ferritic phase and that the austenite remains ductile, see Fig. 7 for an example.

The fracture sequence for the tested base metal specimens at and below −80 °C can be described as ductile until critical cleavage initiation occurred which caused an unstable fracture and thereby failure of the specimen. This indicates that the fracture toughness can be described as the statistical event of critical cleavage initiation, i.e. the weakest link hypothesis [13,14].

The fracture event for the base metal was different compared to hot-rolled plates of 2205 where the cleavage fractures caused delamination which retained the stable fracture process [15,16]. Delamination during fracture toughness testing of duplex hot-rolled plate material has been observed from lean duplex

Table 6
Average chemical composition of the austenite and ferrite in the SAF 2906 base metal.

	Cr (wt%)	Ni (wt%)	Mo (wt%)	Mn (wt%)
Austenite[a]	26.9	8.0	1.6	1.1
Ferrite[a]	28.7	5.9	3.6	0.8

[a] Measured by EDS on ten different spots at different locations for each phase.

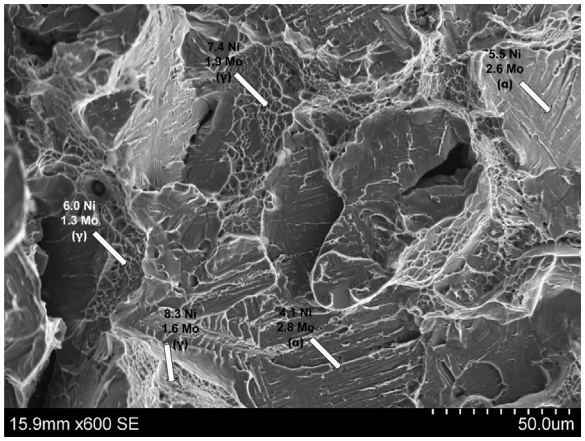

Fig. 7. EDS analysis of the fracture surface. Each analyzed spot is located by a white arrow.

grades [17] to the super duplex grades [18,19]. The cause of the different cleavage fracture propagation is not known but it may be due to the coarser microstructure of the tested SAF 2906 base metal. The average austenite spacing for the SAF 2906 was 26.9 μm compared to 7.0 μm in the 50 mm plate of 2205 that delaminated during testing [15].

Electron backscatter diffraction (EBSD) measurements of the base metal demonstrated that the crystallographic orientation of the ferrite was different in adjacent grains, see Fig. 8. The size of the ferrite grains in the EBSD map was in the same order as the cleavage fracture regions in Fig. 7. This explains the opaque fracture surface, the reflected light was scattered at different angles due to different global cleavage planes.

4.2. The weld metal

The fracture toughness evaluation is based on the assumption that the pre-crack front is straight [8,20]. For the thumbnail-shaped crack front the stress intensity factor (SIF) along the crack front varies. Finite element modeling of thumbnail pre-crack front in compact tension specimens shows that the SIF difference between the deepest region and the shallowest one in a thumbnail pre-crack can be significant [21]. For materials where the unstable fracture is governed by the statistical event of critical cleavage initiation, the initiation does not have to occur in the region of the pre-crack front with the highest SIF. This gives the evaluated fracture toughness for the uneven pre-crack front an uncertainty because it is not known at which SIF the critical cleavage initiation occurred. For the straight pre-crack front the SIF is almost uniform along the pre-crack front [21] which eliminates this uncertainty. For the tested weld metal specimens no correlation between the degree of thumbnail and the fracture toughness could be found. In Fig. 4 in the work by Towers et al. [10] it can be seen that the difference between a straight crack-front and an uneven crack-front (in this case an inverted thumbnail) decreases with decreasing temperature and eventually vanishes. This can be interpreted as that the shape of the pre-crack front is less of importance at the lower shelf temperatures where the toughness is no longer controlled by the statistical event of a critical cleavage initiation [22,23]. This might explain the low scatter in fracture toughness despite the large difference in crack front shapes among the specimens.

If the previous reasoning is valid it is still unclear which crack length to use for evaluating the fracture toughness. A better

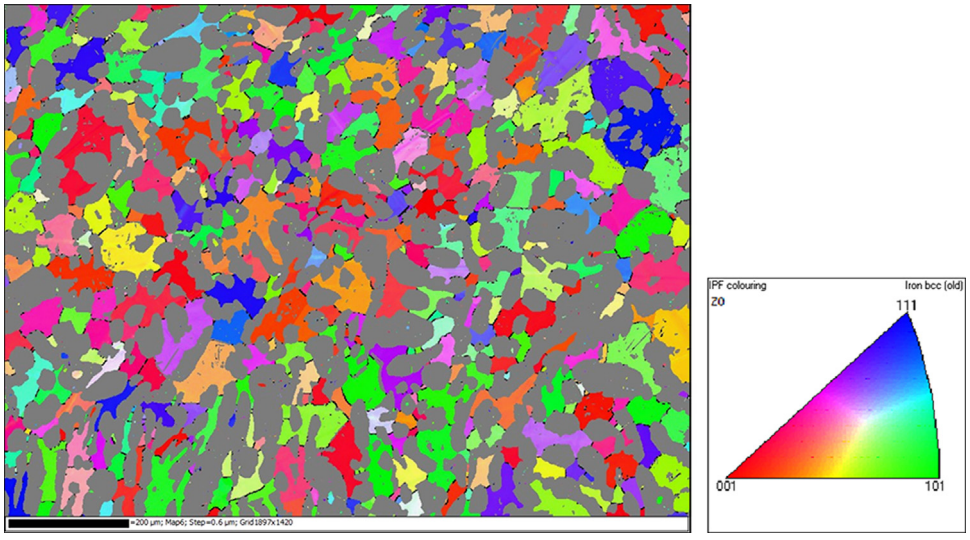

Fig. 8. Inverse pole figure representation of the crystallographic orientation of the ferrite. The gray phase is austenite. EBSD measurement of the SAF 2906 base metal.

Table 7
Substitutional element partitioning in DSS weld metals (standard deviation in parenthesis).

	Phase	Fe (wt%)	Cr (wt%)	Mo (wt%)	Mn (wt%)	Ni (wt%)
LDX 2101® WM [4]	α+γ[a]	66.3 (0.5)	23.5 (0.3)	0.2 (0.03)	1.3 (0.3)	8.1 (0.6)
No. measurement 6	α[b]	65.5 (0.4)	23.9 (0.4)	0.2 (0.2)	1.3 (0.2)	8.3 (0.4)
No. measurement 6	γ[b]	66.3 (0.5)	23.4 (0.5)	0.3 (0.05)	1.4 (0.3)	8.2 (0.5)
LDX 2101® WM [24]	α+γ[a]	68.9 (0.1)	22.4 (1.1)	0.3 (0.03)	1.2 (0.3)	6.1 (0.4)
No. measurement 7	α[b]	68.6 (0.4)	22.6 (0.5)	0.3 (0.1)	1.6 (0.2)	6.2 (0.2)
No. measurement 7	γ[b]	68.8 (0.3)	22.4 (0.3)	0.3 (0.1)	1.7 (0.1)	6.1 (0.2)
2205 WM [5]	α+γ[a]	65.0 (0.1)	22.4 (0.1)	3.0 (0.1)	1.4 (0.01)	7.4 (0.2)
No. measurement 7	α[b]	64.4 (0.3)	22.2 (0.1)	3.5 (0.2)	1.4 (0.03)	7.4 (0.3)
No. measurement 7	γ[b]	65.3 (0.3)	22.1 (0.4)	2.7 (0.2)	1.4 (0.04)	7.9 (0.4)
2906 WM PWHT	α+γ[a]	–	–	–	–	–
No. measurement 14	α[b]	59.5 (0.8)	30.3 (1.2)	3.1 (0.1)	0.5 (0.1)	5.6 (0.3)
No. measurement 13	γ[b]	61.6 (0.5)	28.0 (1.0)	1.4 (0.3)	0.7 (0.04)	7.7 (0.5)
2906 BM PWHT	α+γ[a]	–	–	–	–	–
No. measurement 12	α[b]	59.2 (0.2)	31.9 (0.2)	2.0 (0.1)	0.7 (0.1)	5.3 (0.1)
No. measurement 12	γ[b]	60.1 (0.2)	29.8 (0.2)	1.0 (0.04)	0.7 (0.04)	7.5 (0.1)

[a] EDS, area analysis.
[b] EDS, spot analysis.

approach might be to find the SIF along the crack front (e.g. calculated by FEM software) and the critical fracture initiation. Then a more accurate fracture toughness value could be found. Finding the critical fracture initiation for the tested weld metal specimens was however unsuccessful.

PWHT of duplex stainless steel weldments is not usually done. It can be used to avoid hydrogen cracking when hydrogen pick-up is present, remove large cold deformation or dissolve precipitates detrimental to toughness and corrosion resistance [1]. PWHT for DSS is done at high annealing temperatures to prevent the precipitation of detrimental phases. At these temperatures the diffusion is rapid and the high temperature is likely to change the morphology of the microstructure. As can be seen in Fig. 2b the weld metal lacks the characteristic Widmanstätten austenite and the microstructure was uniform in all directions.

EDS analysis of the chemical content in various DSS weld metals was conducted, see Table 7. The result was that for substitutional elements in as-received weld metals the element partitioning between the phases is minor. For the PWHT specimens in this work the element partitioning was much larger and was close to the base metal.

In a previous work it was shown that high nickel content in the weld metal correlates well with high fracture toughness at sub-zero temperatures [24]. It is therefore suggested that if sub-zero temperature toughness is of importance for the PWHT duplex stainless steel weldment, then further work on the possible influence of element redistribution on the fracture toughness should be carried out.

5. Conclusions

Single-edge notched bend specimens were made from 200 mm diameter bar of the super duplex stainless steel SAF 2906. Both base metal and weld metal specimens were tested to investigate the susceptibility of brittle failure at sub-zero temperatures. The weld metal specimens were heat treated at 1100 °C after welding.

- The tested base metal specimen was fully ductile at −60 °C.
- Between −103 and −80 °C stable fracture occurred for ~200 μm until critical cleavage fracture occurred. This fracture sequence differs from hot-rolled plates of 2205 where cleavage fractures causes delamination which retains a stable fracture process. The cause for the different fracture behavior is not known but may be due to the coarser microstructure.
- The fracture sequence for the heat treated weld metal at −72 °C was critical cleavage fracture initiation after minor crack-tip blunting and ductile fracture. Due to the uneven pre-crack fronts of the specimens no reliable fracture toughness evaluation could be done.
- Post-weld heat treating of DSS weldments can be used for dissolving intermetallic phases and reducing residual stresses which are detrimental to the fracture toughness. However, the results from this work indicate that substitutional element partitioning in the weld metal can occur during PWHT, which leads to reduced nickel content in the ferrite. This may have a negative influence on the fracture toughness at sub-zero temperatures.

Acknowledgments

The authors would like to express their gratitude to the VINN Excellence Center Hero-M and Sandvik Materials Technology for financing this study. Sandvik Materials Technology is also gratefully acknowledged for delivering the material, for performing the EBSD study and for all help.

References

[1] R.N. Gunn, Duplex Stainless Steels – Microstructure, Properties and Applications, Woodhead Publishing Ltd., Abington Hall, 2003.
[2] J. Charles, Revue Métall. 105 (2008) 155–171, http://dx.doi.org/10.1051/metal:2008028.
[3] G. Gedge, J. Const. Steel Res. 64 (11) (2008) 1194–1198.
[4] H Sieurin, E M Westin, M. Liljas, R Sandström, Weld. World 53 (3–4) (2009) R24–R33.
[5] H Sieurin, R Sandström, Eng. Fract. Mech. 73 (2006) 377–390.
[6] ASTM E 1245: Standard Practice for Determining the Inclusion or Second-phase Constituent Content of Metals by Automatic Image Analysis, vol. 03.01.
[7] BS7448 Part 2: Method for Determination of K_{Ic} Critical CTOD and Critical J Values of Welds in Metallic Materials, Seventh Draft (revised), 1996.
[8] ASTM E 1820-06: Standard Test Method for Measurement of Fracture Toughness, vol. 03.01.
[9] ASTM E 1290-08: Standard Test Method for Crack-tip Opening Displacement (CTOD) Fracture Toughness Measurement, vol. 03.01, 2010 ed.
[10] O.L. Towers, M.G. Dawes, Welding Institute Research on the Fatigue Pre-cracking of Fracture Toughness Specimens, Elastic–Plastic Fracture Test Methods: The Users Experience, ASTM STP 856, Ann Arbor, April 1985.
[11] J. Foct, N. Akdut, Scr. Metall. Mater. 29 (1993) 153–158.
[12] R. Lillbacka, G. Chai, M. Ekh, P. Liu, E. Johnson, K. Runesson, Acta Mater. 55 (2007) 5359–5368.
[13] K. Wallin, J. Phys. IV, Colloq. C7, Supp. J. Phys. III 3 (1993) 575–584.
[14] K. Wallin, A. Laukkanen, Eng. Fract. Mech. 75 (2008) 3367–3377.
[15] J. Pilhagen, R. Sandström, Eng. Fract. Mech. 99 (2013) 239–250.
[16] J. Pilhagen, R. Sandström, Metall. Mater. Trans. A 45 (3) (2014) 1327–1337.
[17] H. Sieurin, R. Sandström, E.M. Westin, Metall. Mater. Trans. A 37A (2006) 2975–2981.
[18] C.S. Wiesner, Duplex stainless steels 97, in: Proceedings of 5th World Conference, pp. 979–990.
[19] A. Dhooge, E. Deleu, Stainl. Steel World 7 (1995) 43–51.
[20] J. Zhou, W.O. Soboyejo, Int. J. Fract. 114 (2002) 287–304.
[21] L. Alverlind, Inflytande av sprickform vid spänningskorrosiv provning (in English: influence of the crack shape on stress corrosion testing) (M.Sc. thesis), Department of Solid Mechanics, KTH Royal Institute of Technology, Stockholm, Sweden, 2003.
[22] K. Wallin, J. Phys. IV 3 (1993) 575–584.
[23] K. Wallin, Int. J. Mater. Prod. Technol. 14 (2/3/4) (1999) 342–353.
[24] J. Pilhagen, R. Sandström, Mater. Sci. Eng. A 602C (2014) 49–57.